Extreme Rapid Intensification of Typhoon Vicente (2012) in the South China Sea

OWEN H. SHIEH

National Disaster Preparedness Training Center, Honolulu, Hawaii

MICHAEL FIORINO

NOAA/Earth System Research Laboratory, Boulder, Colorado

MATTHEW E. KUCAS

Joint Typhoon Warning Center, Pearl Harbor, Hawaii

BIN WANG

Department of Meteorology, University of Hawai'i at Mānoa, Honolulu, Hawaii

(Manuscript received 28 June 2013, in final form 29 August 2013)

ABSTRACT

One of the primary challenges for both tropical cyclone (TC) research and forecasting is the problem of intensity change. Accurately forecasting TC rapid intensification (RI) is particularly important to interests along coastlines and shipping routes, which are vulnerable to storm surge and heavy seas induced by intense tropical cyclones. One particular RI event in the western North Pacific Ocean with important scientific implications is the explosive deepening of Typhoon Vicente (2012). Vicente underwent extreme RI in the northern South China Sea just prior to landfall west of Hong Kong, China, with maximum sustained winds increasing from 50 kt (1 kt = 0.51 m s^{-1}) at 0000 UTC 23 July to 115 kt at 1500 UTC 23 July. This increase of 65 kt in 15 h far exceeds established thresholds for TC RI. Just prior to this RI episode, Vicente exhibited a near-90° poleward track shift. The relationship between the track and intensity change is described, and the authors speculate that the passage of an upper-tropospheric (UT) "inverted" trough was a significant influence. An analysis of real-time numerical model guidance is provided and is discussed from an operational perspective, and high-resolution global model analyses are evaluated. Numerical model forecasts of the UT trough interaction with the TC circulation were determined to be a shortcoming that contributed to the intensity prediction errors for Vicente. This case study discusses the importance of considering UT features in TC intensity forecasting and establishes current modeling capabilities for future research.

1. Introduction

This paper documents the extreme rapid intensification (RI) of Typhoon Vicente, the ninth tropical cyclone (TC) of the 2012 western North Pacific Ocean (WPAC) typhoon season, based on the Joint Typhoon Warning Center (JTWC) best-track record. Given the pressing need for advancements in TC intensity forecast skill and the broad interest in this exceptional case of TC RI, we summarize the evolution and real-time numerical model forecast errors of Vicente to establish a baseline for future research.

The objectives of TC prediction are to skillfully and reliably forecast the track, intensity, and evolution of the TC surface wind field and its associated impacts. While mean TC track forecast errors have decreased in recent decades, both numerical and subjective predictions of TC intensity have shown minimal improvements (DeMaria et al. 2007). TC intensity change is generally considered to be governed by 1) synoptic and large-scale environmental factors (e.g., 850–200-hPa vertical wind shear), 2) internal dynamics within the TC circulation (e.g., eyewall replacement cycles), and

Corresponding author address: Owen Shieh, National Disaster Preparedness Training Center, 828 Fort Street Mall, Ste. 320, Honolulu, HI 96813.
E-mail: oshieh@hawaii.edu

DOI: 10.1175/WAF-D-13-00076.1

3) processes at the ocean–atmosphere interface (Bosart et al. 2000). However, these factors often act in opposition, rendering rapid fluctuations in TC intensity difficult to forecast.

Although warm sea surface temperatures (SSTs) and upper-ocean heat content (OHC) are known to favor TC intensification (e.g., Lin et al. 2008), mesoscale variations in subsurface thermal structure are usually difficult to observe in real time. Furthermore, large-scale oceanic conditions often satisfy the necessary—albeit not always sufficient—condition for TC intensification within WPAC TC-development regions. Thus, while a subjective assessment of oceanic thermal structure is part of the operational TC forecast process in the WPAC, forecasters focus on the more readily observable atmospheric conditions.

Holland and Merrill (1984) discussed the sensitivity of TC structure and intensity to upper-tropospheric (UT) influences due to the lower inertial stability aloft within a TC vortex, which can be described by eddy angular momentum flux convergence (e.g., DeMaria et al. 1993). For example, UT radial outflow channels have been known to modulate TC intensity (e.g., Chen and Gray 1985). These UT outflow patterns may be influenced by UT low pressure systems that are cut off from the midlatitude flow or embedded within the climatological tropical upper-tropospheric trough (TUTT) as ''TUTT cells'' (TUTTcs), first described by Sadler (1975, 1976). Several observational studies have documented the interaction of TCs with UT troughs (Rodgers et al. 1991; DeMaria et al. 1993; Bosart et al. 2000), and composite studies in the Atlantic (Hanley et al. 2001) and WPAC (Ventham and Wang 2007) have suggested that UT trough interaction can affect TC intensity. Numerical studies (Shi et al. 1997; Kimball and Evans 2002) identified relationships between TC intensity change and the structure of nearby UT troughs. However, questions still remain with regard to UT influences on TC intensity, particularly those associated with TUTTcs.

In addition to the challenge of understanding the dynamical mechanisms that drive RI, many criteria have been proposed to quantify TC RI. Holliday and Thompson (1979) defined RI in the WPAC as a deepening of the minimum central pressure by 42 hPa in 24 h, while more recently, Kaplan and DeMaria (2003) defined RI in the Atlantic as an increase in maximum sustained 1-min surface average wind speed of 30 kt ($1\ \mathrm{kt} = 0.51\ \mathrm{m\,s^{-1}}$) in 24 h. This latter definition has been frequently cited in both research and forecast applications and is recognized as the standard for RI in all ocean basins. However, Ventham and Wang (2007) found that the frequency and subsequent potential of RI is actually a function of initial TC intensity, but for the sake of simplicity, an acceptable RI definition for all TCs in the WPAC was proposed by Wang and Zhou (2008) as an increase of maximum sustained winds of 30 kt in 24 h, with a minimum 5-kt increase in the first 6 h and a 10-kt increase in the first 12 h of the RI period.

Several aspects of Typhoon Vicente are noteworthy. The storm was the strongest typhoon to affect the Hong Kong metropolitan area since Typhoon York in 1999, and it underwent RI over the northern South China Sea just prior to landfall. Although climatological TC occurrence over that area is comparable to the rate of occurrence in the Philippine Sea, RI is observed much less frequently (e.g., Wang and Zhou 2008). Typhoon Vicente underwent an estimated 65-kt increase in maximum sustained winds within 15 h, far exceeding established RI thresholds and was only the second occurrence of such extreme RI since 1979 in the South China Sea. Vicente also exhibited an interesting relationship between track and intensity, with a near-90° right turn to the north occurring immediately before RI. Global and regional numerical models did not predict this track and intensity change, perhaps due in part to inadequate analyses and forecasts of the UT flow.

2. Numerical models and observational data

While a large suite of global and regional, dynamical, and statistical–dynamical numerical models are available to JTWC, forecasters typically follow a consensus of global dynamical TC vortex trackers, rather than any individual model forecast (Goerss 2000). The primary WPAC consensus (CONW) used at JTWC in 2012 was an average of forecast tracks from the following models: 1) the National Centers for Environmental Prediction (NCEP) Global Forecast System (GFS), 2) the European Centre for Medium-Range Weather Forecasts model (ECMWF), 3) the Met Office model (UKMET), 4) the Navy Operational Global Atmospheric Prediction System, 5) the Japan Global Spectral Model, 6) the U.S. Navy's version of the Geophysical Fluid Dynamics Laboratory hurricane model (GFDN), and 7) the Weber barotropic model (WBAR; Sampson et al. 2006). For operational use, the forecast tracks of the most recent runs of these models were interpolated 6 and sometimes 12 h forward in time to match the time and location of the JTWC warning position. A more in-depth discussion of the interpolation process with citations for CONW dynamical model guidance can be found in Goerss et al. (2004) and Payne et al. (2007).

Currently at the JTWC the most skillful TC intensity forecasts blend statistical–dynamical schemes, such as the Statistical Typhoon Intensity Prediction Scheme (Knaff et al. 2005), with deterministic forecasts from

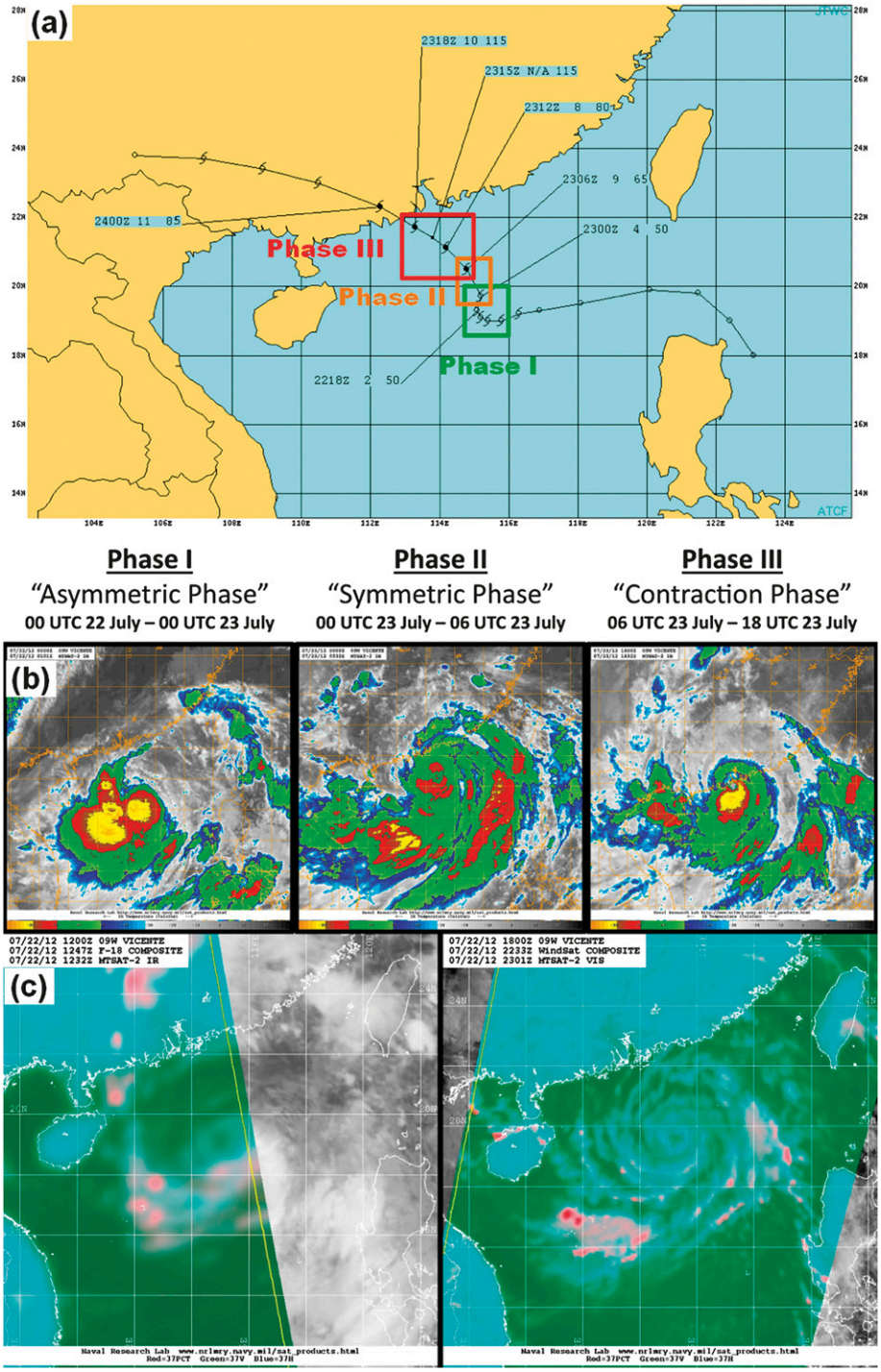

FIG. 1. (a) JTWC best track for Typhoon Vicente adapted from Fig. 1-19 in Evans and Falvey (2012). Open circles indicate tropical depression intensity, open tropical cyclone symbols indicate tropical storm intensity, and closed tropical cyclone symbols indicate typhoon intensity. Track labels indicate date and time (UTC), translational speed (kt), and maximum sustained winds (kt). (b) Sequential *MTSAT-2* infrared imagery (0101 UTC 22 Jul, 0532 UTC 23 Jul, and 1832 UTC 23 Jul) representative of each of the three phases of Typhoon Vicente's RI. These phases are also indicated in the best-track data in (a). Each panel of (b) is approximately centered on the LLCC. (c) Color-composited 37-GHz microwave satellite imagery from (left) Special Sensor Microwave Imager/Sounder (SSMIS) at 1247 UTC 22 Jul and (right) WindSat at 2233 UTC 22 Jul.

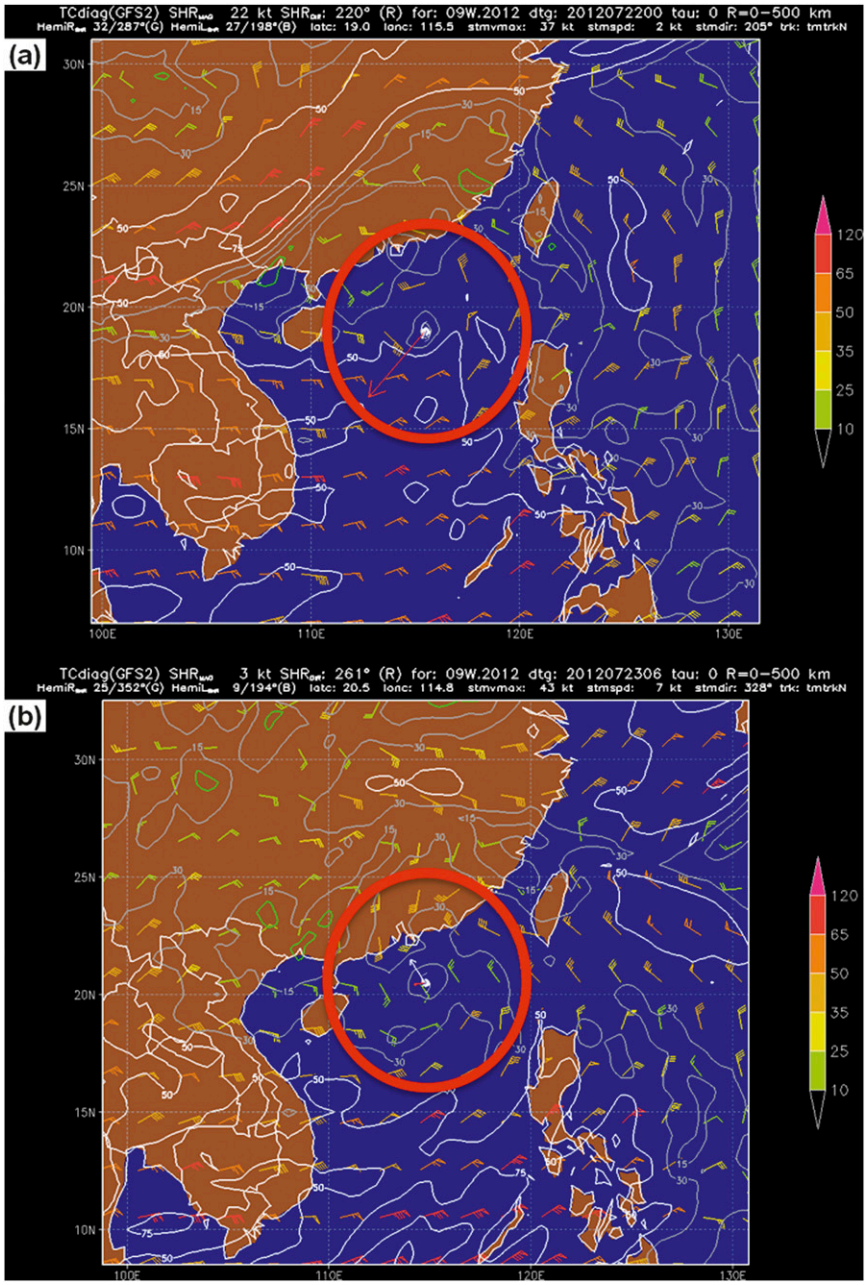

FIG. 2. WxMap2 TCdiag 0.5° GFS analysis at (a) 0000 UTC 22 Jul and (b) 0600 UTC 23 Jul, showing 200–850-hPa vertical wind shear at each location (wind barbs) and the resultant average vertical wind shear vector (red arrow). The average vertical wind shear is the difference between the area-averaged (radius r = 0–500 km within red circle) 200- and 850-hPa winds. Also shown is the TC forward motion vector (white arrow). Contours indicate vertical wind shear magnitude (kt).

high-resolution dynamical models. JTWC also considers individual forecasts from a suite of mesoscale models, including the GFDN (Rennick 1999), the Hurricane Weather Research and Forecasting model (HWRF; Gopalakrishnan et al. 2010), the Coupled Ocean–Atmosphere Mesoscale Prediction System for Tropical Cyclones (COAMPS-TC; Hendricks et al. 2011), and the U.S. Air Force Weather Agency Mesoscale Ensemble Prediction System (Hacker et al. 2011). Intensity guidance under development includes a consensus of

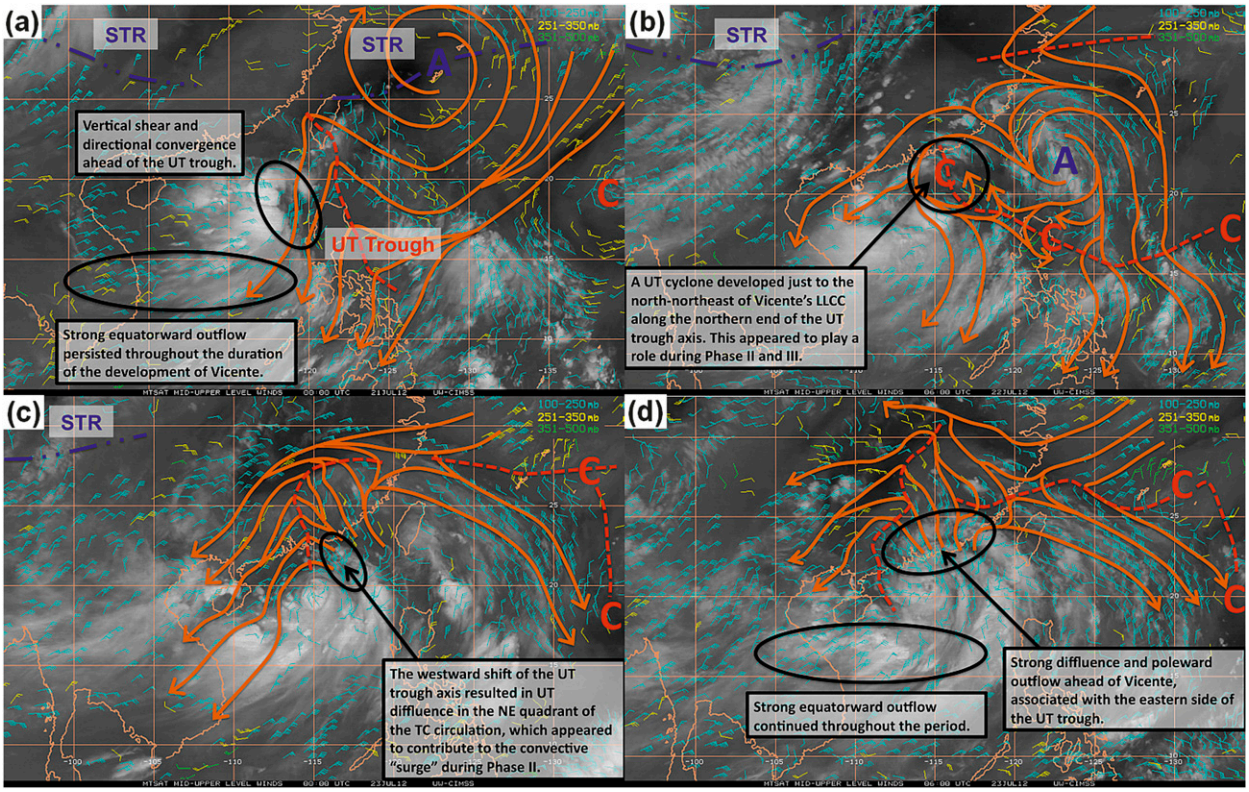

FIG. 3. Annotated *MTSAT-2* water vapor imagery with CIMSS satellite-derived mid- to upper-tropospheric wind barbs at (a) 0000 UTC 21 Jul, (b) 0600 UTC 22 Jul, (c) 0000 UTC 23 Jul, and (d) 0600 UTC 23 Jul. Schematic annotations include subjectively analyzed streamlines (orange arrows), STR axes (blue dashed and dotted lines), UT trough axes (red dashed lines), cyclonic circulation centers (red "C"), and anticyclonic circulation centers (blue "A"). Note the presence and structure of the UT trough in all panels. Although this paper describes the influence of the UT trough on the structure and intensity of Vicente, the interaction between the two systems may have altered the structure of the UT trough as well.

forecasts from the Logistic Growth Equation Model (DeMaria 2009) and Statistical Hurricane Intensity Prediction System applied to the WPAC (Evans and Falvey 2012, p. 4).

A variety of satellite data was available for this case study: 1) satellite imagery from the Japanese *Multifunctional Transport Satellite-2* (*MTSAT-2*) was obtained from archives at the Naval Research Laboratory in Monterey, California, and 2) satellite-derived wind analyses were obtained from the University of Wisconsin—Madison Cooperative Institute for Meteorological Satellite Studies (CIMSS). The JTWC final best track and real-time numerical-model forecast tracks for Typhoon Vicente were plotted using the operational Automated Tropical Cyclone Forecasting system. Global model gridded fields [0.5° GFS from NCEP and 0.5° ECMWF from The Observing System Research and Predictability Experiment Interactive Grand Global Ensemble (TIGGE) server] were analyzed using the WxMap2 TCdiag numerical model analysis and visualization Internet site (http://ruc.noaa.gov/hfip/tcdiag/09w.php).

3. Evolution of Typhoon Vicente

Typhoon Vicente originated as a convective disturbance embedded within the monsoon trough just to the east of Luzon in the Philippines on 18 July 2012. As multiple vortices consolidated around a single low-level circulation center (LLCC), the developing cyclone tracked westward, steered by the deep-layer flow south of the subtropical ridge (STR) until the first warning was issued at 0000 UTC 21 July (Evans and Falvey 2012, 54–60). On 22 July, Vicente abruptly turned northward around 1800 UTC 22 July (Fig. 1a). A period of RI immediately followed this track shift, with maximum sustained winds increasing from 50 kt at 0000 UTC 23 July to 115 kt at 1500 UTC 23 July, an increase of 65 kt in 15 h. Vicente made landfall at 2100 UTC 23 July approximately 70 n mi (~130 km) west of Hong Kong, with its intensity estimated to be near 100 kt.

To better illustrate the dynamics that drove the abrupt track and intensity changes, the evolution of Vicente is divided into three phases (Fig. 1b): phase I, or the

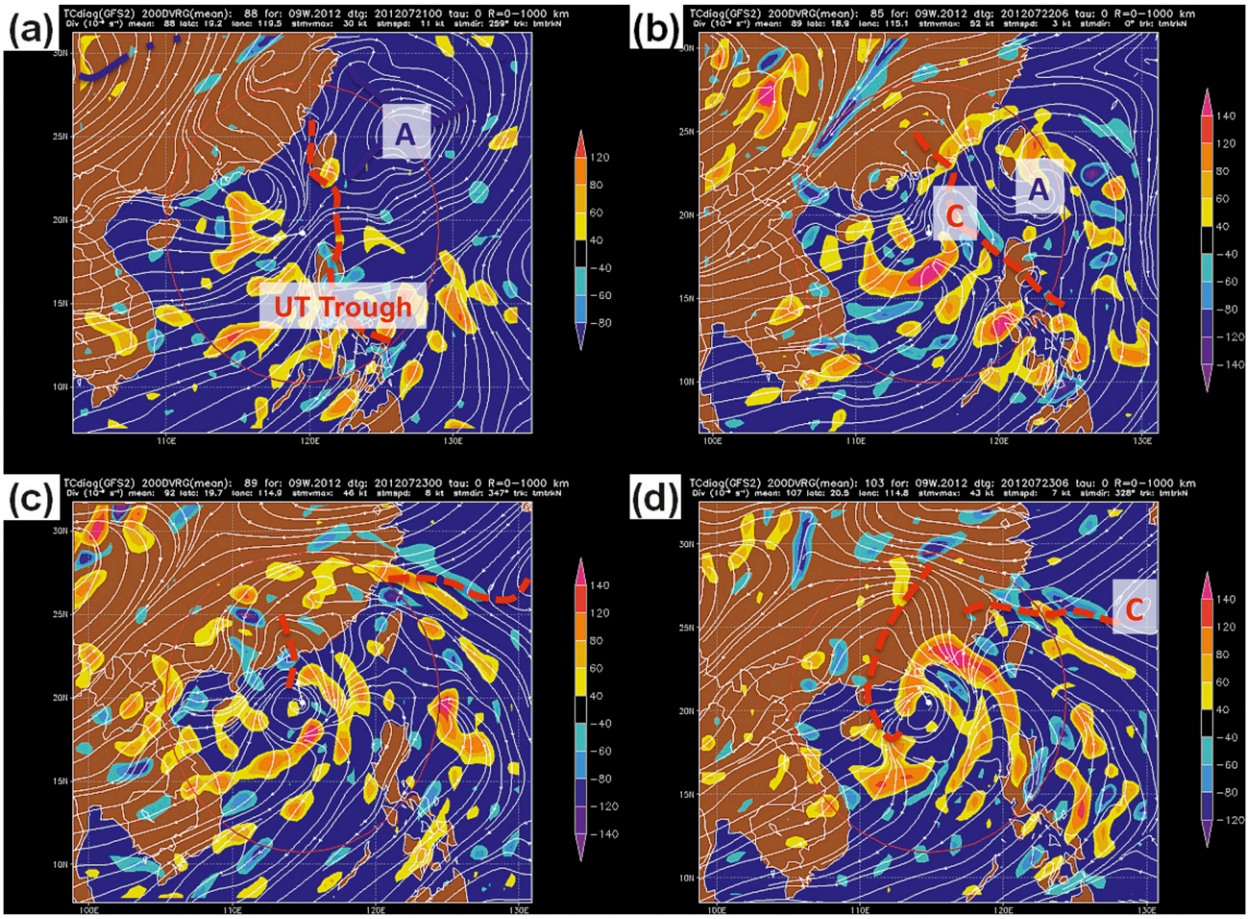

FIG. 4. The 200-hPa 0.5° GFS analyses corresponding to the same times as in Fig. 3, showing objectively analyzed streamlines (white lines with arrows), model-analyzed divergence ($10^{-6}\,s^{-1}$) (shaded colors; right legend), and TC forward motion vector (white arrow) (kt). The red circle marks a radius of $r = 1000$ km from the TC center. Relevant synoptic features are annotated as in Fig. 3.

asymmetric phase (0000 UTC 22 July–0000 UTC 23 July); phase II, the symmetric phase (0000–0600 UTC 23 July), and phase III, the contraction phase (0600–1800 UTC 23 July). Phase I was characterized by persistent moderate-to-strong northeasterly vertical shear of greater than 20 kt across Vicente (Fig. 2a). The effect of this shear was evident as a wavenumber-1 asymmetry in the convective pattern (left panel of Fig. 1b), with periodic bursts of deep convection in the downshear-left quadrant, consistent with previous studies of TC vortex secondary circulation response to vertical wind shear (e.g., Corbosiero and Molinari 2002). Furthermore, 37-GHz microwave imagery indicated a closed, low-level ring pattern as early as 1247 UTC (see Kieper and Jiang 2012), with significant banding evident by 2233 UTC (Fig. 1c), suggesting the potential for RI. By 0600 UTC 23 July, RI was well under way, with vertical wind shear decreasing to less than 5 kt (Fig. 2b) in association with a rapid axisymmetrization of the TC convection. Most of the intensification occurred prior to the local diurnal convective maximum, suggesting that ambient environmental conditions played a significant role in this RI episode. During the remainder of the RI period prior to landfall, central convection increased rapidly, with a symmetric ring of cold cloud tops developing around the eye, and a contraction of the convective envelope of the circulation during phase III.

During the day prior to phase I, a weakness in the STR that is due to a UT "inverted" trough extended from the vicinity of Luzon to southern Taiwan (Figs. 3a and 4a). Northeasterly shear, directional convergence, and associated subsidence induced by the UT trough contributed to the lack of convection to the east and northeast of the LLCC. As the steering influence of the STR began to weaken, the UT trough axis continued westward and became embedded within the outflow envelope of Vicente (Figs. 3b,c and Figs. 4b,c). Strong equatorial outflow persisted throughout this period,

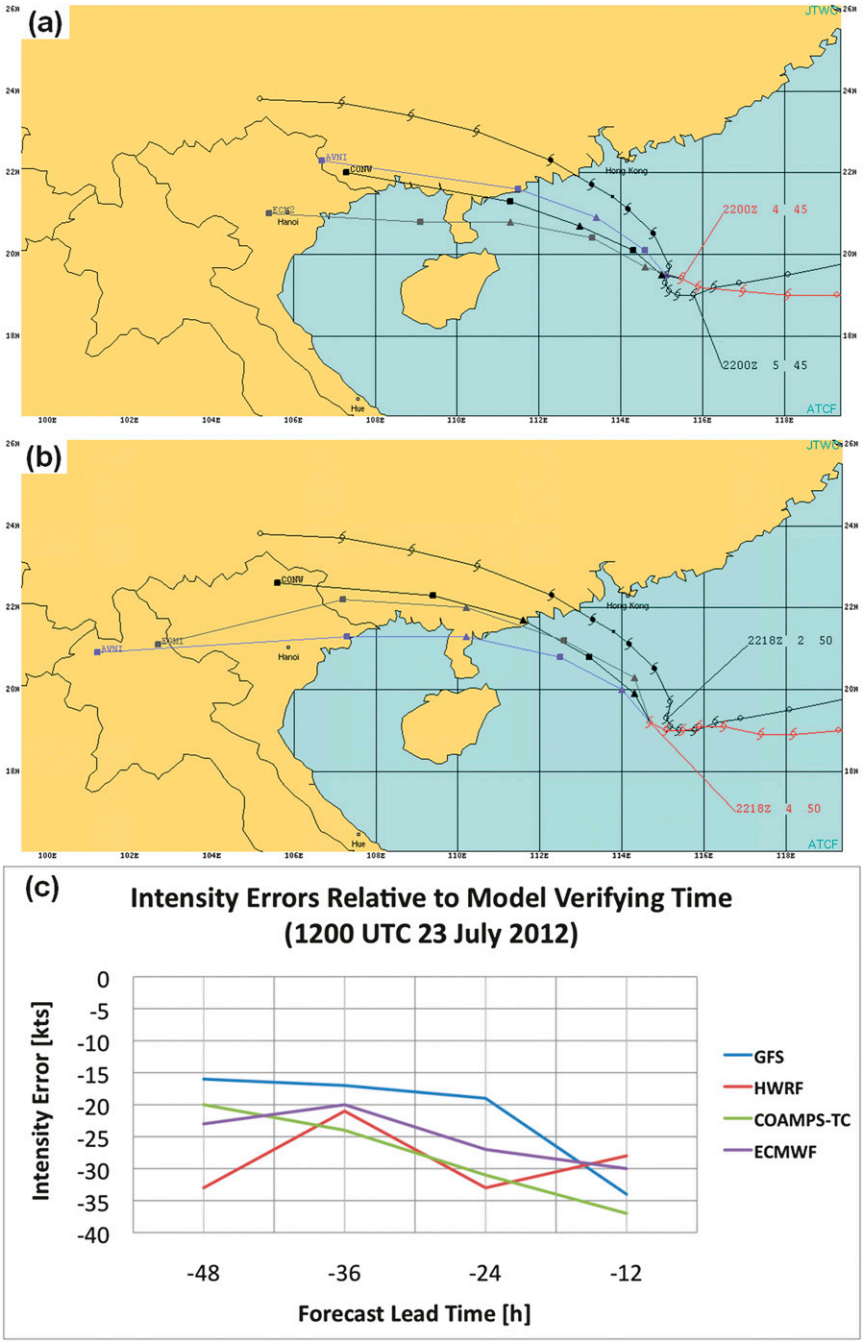

FIG. 5. (a) JTWC final best track (black) and the real-time best track prior to poststorm analysis (red) with positions and labels as in Fig. 1. Primary objective numerical model track forecasts from the 6-h interpolation GFS (AVNI), 12-h interpolation ECMWF (ECM2), and consensus (CONW) at 0000 UTC 22 Jul. (b) As in (a), but with the 6-h interpolation ECMWF (ECMI) and at 1800 UTC 22 Jul. (c) Time series of intensity forecast errors for GFS, HWRF, COAMPS-TC, and ECMWF with respect to individual forecast lead times for the verifying time of 1200 UTC 23 Jul.

enabling Vicente to maintain intensity despite the presence of strong vertical wind shear. By 0000 UTC 23 July, the axis passed to the west of Vicente's LLCC, causing northeasterly, radially convergent UT inflow to abruptly make a transition to southeasterly, divergent outflow. This shift in the UT flow pattern resulted in the rapid reduction of northeasterly shear while simultaneously establishing UT divergence in the northeastern quadrant

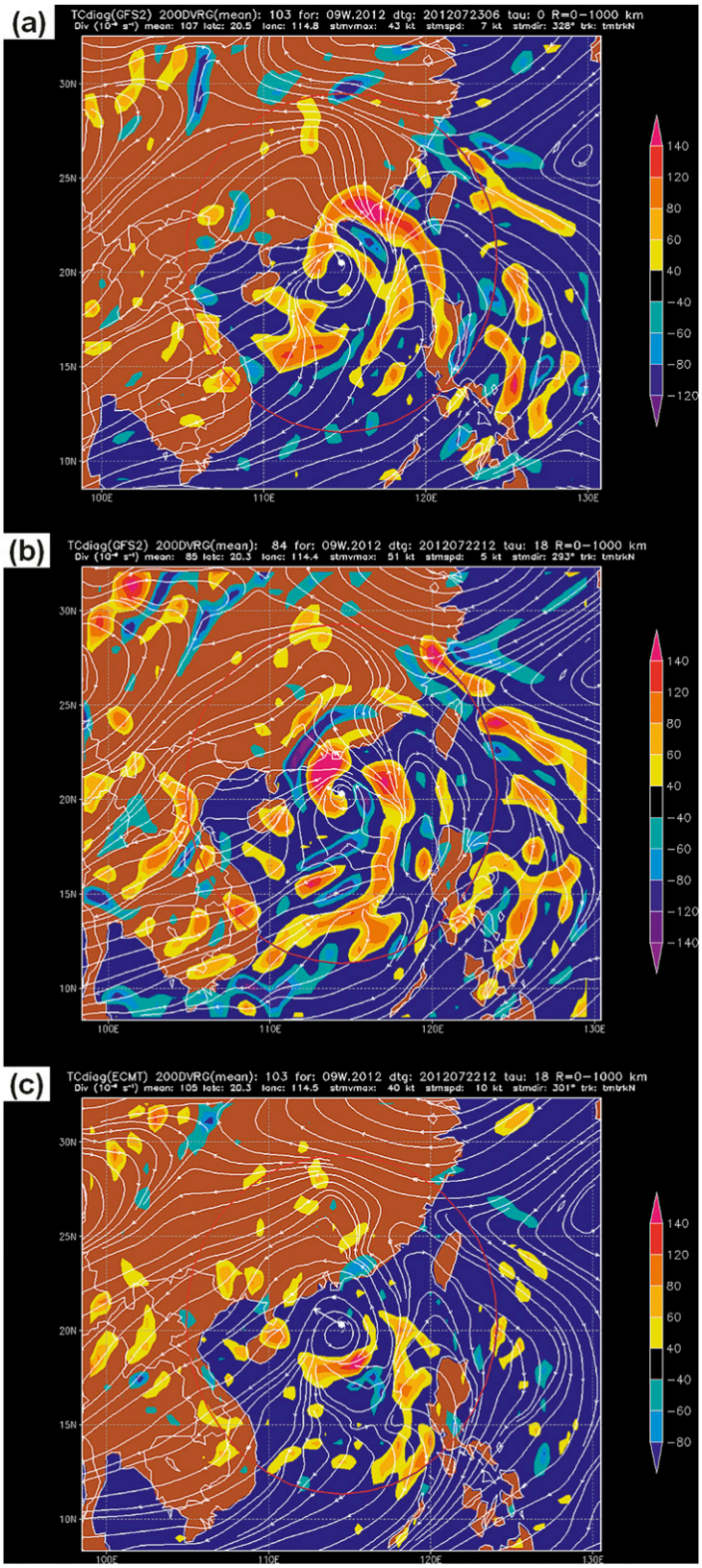

FIG. 6. Plots of 200-hPa divergence as in Fig. 4, with (a) GFS analysis valid at 0600 UTC 23 Jul (reproduction of Fig. 4d). (b) The 18-h GFS forecast verifying at 0600 UTC 23 Jul. (c) As in (b), but for ECMWF.

(Figs. 3c and Figs. 4c). Coincident with the change in the UT flow was a shift in the midlevel steering flow to southerlies. Furthermore, pressure falls induced by the deep convection north of the center may have caused the surface center to shift or reform. These factors likely contributed to the northward turn of Vicente and the subsequent convective surge in phase II. As the UT trough axis continued westward, Vicente remained under a favorable poleward and equatorward outflow regime (Figs. 3d and 4d), thus allowing RI to proceed unimpeded until landfall.

4. Numerical model forecast errors

The difficulty of forecasting RI is well known (e.g., Kucas 2010), but Vicente posed an additional challenge with its abrupt poleward track shift that was missed by the numerical models used in CONW, which were consistently biased westward during the model runs prior to 0000 UTC 22 July (Fig. 5a). It was not until 1800 UTC 22 July, after Vicente began the turn to the north, that CONW shifted northward, but even this latter prediction suggested that Vicente would track farther to the west than was eventually observed (Fig. 5b). Intensity prediction errors for all of the dynamical models were consistently negative and did not improve with shorter forecast times (Fig. 5c). For the 1200 UTC 23 July verifying time, the global models (GFS and ECMWF) had lower 48-h forecast intensity errors than HWRF, suggesting that the model physics that affected the TC intensification rate was a more important factor than were the initial conditions, whereas the 12-h HWRF forecast may have benefited from a better analysis of the TC vortex. The magnitude of the errors verifying at the peak intensity on 1800 UTC 23 July was much larger (not shown) at all forecast times, as neither the initial vortex nor the model physics could produce the extreme intensification.

The 0600 UTC 23 July GFS analysis depicted strong divergence to the northeast of Vicente wrapping into the center ahead of the storm (Fig. 6a), thus favoring intensification. Both the GFS (Fig. 6b) and ECMWF (Fig. 6c) simulations failed to capture the structure of the UT trough at an 18-h forecast time, with ECMWF underforecasting the magnitude of the 200-hPa diffluence/divergence (Fig. 5c). Forecasts of the UT trough structure at longer forecast times (not shown) were even less accurate, consistent with shortcomings noted by Patla et al. (2009).

5. Summary and discussion

Typhoon Vicente was an exceptional case of RI, with the cyclone undergoing a 65-kt increase in maximum sustained winds within 15 h. This rapid deepening was preceded by an abrupt, northward track shift. Operational numerical models predicted neither RI nor the track shift. The weakening of the steering STR possibly in response to the passage of a UT trough, the associated decrease in vertical wind shear and resultant poleward shift in steering flow, and subsequent increase in UT divergence all appeared to have contributed to the timing of the rapid shift in Typhoon Vicente's track and the subsequent RI. Satellite and global model analyses provide evidence in support of this hypothesis.

Although the Kieper and Jiang (2012) method suggested the 30-kt increase in intensity from 1200 UTC 22 July through 1200 UTC 23 July, there are currently no reliable tools that could have captured the extreme RI that continued through the subsequent 6-h period. According to Evans and Falvey (2012, 54–60), there were no operationally significant changes to SSTs and OHC along the path of Vicente that would have hinted at such extreme RI, so we speculate that the UT environment was of primary importance in this case. The need to clarify the dynamics behind TC interactions with UT troughs and TUTTcs cannot be understated. We believe that modern high-resolution global numerical model analyses can be used to quantify the competing influences of vertical wind shear and UT divergence. To achieve this, we are developing an objective TUTTc tracker that can better quantify the nature of UT–TC interactions.

Acknowledgments. Financial support was provided by NASA Award NNX09AG97G and O. Shieh's NSF Graduate Research Fellowship. M. Fiorino's contribution was supported by the NOAA/Hurricane Forecast Improvement Project. We thank Ramona Ferreyra and Marcela Gill, formerly at U.S. Pacific Command at Camp H. M. Smith, for facilitating the JTWC collaboration. Finally, we acknowledge JTWC Commanding Officer Capt. Ashley Evans, USN, Director Robert Falvey, and the current and former JT Operations Officers Lt. Chad Geis, USN, and Lt. Cdr. Sarah Follett, USN, for supporting O. Shieh's Typhoon Duty Officer training.

REFERENCES

Bosart, L. F., W. E. Bracken, J. Molinari, C. S. Velden, and P. G. Black, 2000: Environmental influences on the rapid intensification of Hurricane Opal (1995) over the Gulf of Mexico. *Mon. Wea. Rev.,* **128,** 322–352.

Chen, L., and W. M. Gray, 1985: Global view of the upper level outflow patterns associated with tropical cyclone intensity changes during FGGE. Colorado State University Dept. of Atmospheric Science Paper 392, 126 pp.

Corbosiero, K. L., and J. Molinari, 2002: The effects of vertical wind shear on the distribution of convection in tropical cyclones. *Mon. Wea. Rev.,* **130,** 2110–2123.

DeMaria, M., 2009: A simplified dynamical system for tropical cyclone intensity prediction. *Mon. Wea. Rev.,* **137,** 68–82.

——, J. Kaplan, and J.-J. Baik, 1993: Upper-level eddy angular momentum fluxes and tropical cyclone intensity change. *J. Atmos. Sci.,* **50,** 1133–1147.

——, J. A. Knaff, and C. Sampson, 2007: Evaluation of long-term trends in tropical cyclone intensity forecasts. *Meteor. Atmos. Phys.,* **97,** 19–28.

Evans, A. D., and R. J. Falvey, 2012: Annual tropical cyclone report 2012. Joint Typhoon Warning Center Rep., 117 pp. [Available online at http://www.usno.navy.mil/NOOC/nmfc-ph/RSS/jtwc/atcr/2012atcr.pdf.]

Goerss, J. S., 2000: Tropical cyclone track forecasts using an ensemble of dynamical models. *Mon. Wea. Rev.,* **128,** 1187–1193.

——, C. R. Sampson, and J. M. Gross, 2004: A history of western North Pacific tropical cyclone track forecast skill. *Wea. Forecasting,* **19,** 633–638.

Gopalakrishnan, S. G., Q. Liu, T. Marchok, D. Sheinin, N. Surgi, R. Tuleya, R. Yablonsky, and X. Zhang, 2010: Hurricane Weather and Research and Forecasting (HWRF) model scientific documentation. NOAA/NCAR/Development Tech Center Doc., 75 pp. [Available online at http://www.dtcenter.org/HurrWRF/users/docs/scientific_documents/HWRF_final_2-2_cm.pdf.]

Hacker, J. P., and Coauthors, 2011: The U.S. Air Force Weather Agency's mesoscale ensemble: Scientific description and performance results. *Tellus,* **63A,** 625–641.

Hanley, D., J. Molinari, and D. Keyser, 2001: A composite study of the interactions between tropical cyclones and upper-tropospheric troughs. *Mon. Wea. Rev.,* **129,** 2570–2584.

Hendricks, E. A., M. S. Peng, X. Ge, and T. Li, 2011: Performance of a dynamic initialization scheme in the Coupled Ocean–Atmosphere Mesoscale Prediction System for Tropical Cyclones (COAMPS-TC). *Wea. Forecasting,* **26,** 650–663.

Holland, G. J., and R. T. Merrill, 1984: On the dynamics of tropical cyclone structural changes. *Quart. J. Roy. Meteor. Soc.,* **110,** 723–745.

Holliday, C. R., and A. H. Thompson, 1979: Climatological characteristics of rapidly intensifying typhoons. *Mon. Wea. Rev.,* **107,** 1022–1034.

Kaplan, J., and M. DeMaria, 2003: Large-scale characteristics of rapidly intensifying tropical cyclones in the North Atlantic basin. *Wea. Forecasting,* **18,** 1093–1108.

Kieper, M. E., and H. Jiang, 2012: Predicting tropical cyclone rapid intensification using the 37 GHz ring pattern identified from passive microwave measurements. *Geophys. Res. Lett.,* **39,** L13804, doi:10.1029/2012GL052115.

Kimball, S. K., and J. L. Evans, 2002: Idealized numerical simulations of hurricane–trough interaction. *Mon. Wea. Rev.,* **130,** 2210–2227.

Knaff, J. A., C. R. Sampson, and M. DeMaria, 2005: An operational statistical typhoon intensity prediction scheme for the western North Pacific. *Wea. Forecasting,* **20,** 688–699.

Kucas, M. E., 2010: Challenges of forecasting tropical cyclone intensity change at the Joint Typhoon Warning Center. Preprints, *29th Conf. on Hurricanes and Tropical Meteorology,* Tucson, AZ, Amer. Meteor. Soc., 9C.6. [Available online at https://ams.confex.com/ams/pdfpapers/168732.pdf.]

Lin, I. I., C.-C. Wu, I.-F. Pun, and D.-S. Ko, 2008: Upper-ocean thermal structure and the western North Pacific category 5 typhoons. Part I: Ocean features and the category 5 typhoons' intensification. *Mon. Wea. Rev.,* **136,** 3288–3306.

Patla, J. E., D. Stevens, and G. M. Barnes, 2009: A conceptual model for the influence of TUTT cells on tropical cyclone motion in the northwest Pacific Ocean. *Wea. Forecasting,* **24,** 1215–1235.

Payne, K. A., R. L. Elsberry, and M. A. Boothe, 2007: Assessment of western North Pacific 96- and 120-h track guidance and present forecastability. *Wea. Forecasting,* **22,** 1003–1015.

Rennick, M. A., 1999: Performance of the navy's tropical cyclone prediction model in the western North Pacific basin during 1996. *Wea. Forecasting,* **14,** 297–305.

Rodgers, E. B., S. W. Chang, J. Stout, J. Steranka, and J.-J. Shi, 1991: Satellite observations of variations in tropical cyclone convection caused by upper-tropospheric troughs. *J. Appl. Meteor. Climatol.,* **30,** 1163–1184.

Sadler, J. C., 1975: The upper tropospheric circulation over the global tropics. University of Hawaii Dept. of Meteorology Rep. UHMET-75-05, 35 pp.

——, 1976: A role of the tropical upper tropospheric trough in early season typhoon development. *Mon. Wea. Rev.,* **104,** 1266–1278.

Sampson, C. R., J. S. Goerss, and H. C. Weber, 2006: Operational performance of a new barotropic model (WBAR) in the western North Pacific basin. *Wea. Forecasting,* **21,** 656–662.

Shi, J. J., S. Chang, and S. Raman, 1997: Interaction between Hurricane Florence (1988) and an upper-tropospheric westerly trough. *J. Atmos. Sci.,* **54,** 1231–1247.

Ventham, J. D., and B. Wang, 2007: Large-scale flow patterns and their influence on the intensification rates of western North Pacific tropical storms. *Mon. Wea. Rev.,* **135,** 1110–1127.

Wang, B., and X. Zhou, 2008: Climate variation and prediction of rapid intensification in tropical cyclones in the western North Pacific. *Meteor. Atmos. Phys.,* **99,** 1–16.